S. Ergul*, M. Akyildiz*, A. Karamanov**

Ceramic material from basaltic tuffs

The possibility to obtain a cheap ceramic material based on 50 wt % basaltic tuffs and 50 wt % industrial clays was studied. The tuffs were characterized by optical microscopy, X-ray diffraction and differential thermal analysis. It was shown that this material is appropriate for the ceramic industry: it is easy for milling and is characterized by low liquidus temperature. The sintering behaviour of the ceramic was evaluated by hot-stage microscopy and dilatometry. The structure of samples, heat-treated at different temperatures, were observed by scanning electron microscopy while the densification degree was evaluated by dry flow and gas pycnometery. Samples with 13% total porosity and 4% water absorption were obtained at 1150 °C for 30 min soaking.

Main Author

Curriculum

1. Introduction

Feldspars, quartz and clays are the base of the ceramic industry[1-5]. The clays give plasticity on the body for shaping, the feldspars favour liquid phase formation and densification at low temperature while the sands reduce distortion and shrinkage.

Last decades, however, several new raw materials or different industrial wastes have been introduced in the batch compositions[6-14]. These materials are mainly used instead of the feldspars, which are the most expensive part of the common ceramic batch.

Also, some ancient ceramics may be considered as alternative compositions. An interesting example could be the pottery samples from the Byzantium period, found in Southern Anatolia[15-17]. The mineralogical analysis of these terra-cotta sculptures highlights the use of local basaltic tuffs.

In this region of Turkey the volcanism is well studied[18-19]. It was demonstrated that these igneous rocks come from the Plio-Quaternary age and are characterized by OIB (ocean island basalts) compositions. The total reserve of the tuff deposits is estimated as about 1000 Mt. It was also found that the chemical and mineralogical compositions show negligible variations.

The basaltic rocks belong to several groups according to the $(SiO_2 + Al_2O_3)/(Na_2O + K_2O)$ ratio. The most common are the tholeiite and the alkali

* *Department of Geological Engineering, University of Cukurova, Balcali, Adana, Turkey; ** Institute of Physical Chemistry, Bulgarian Academy of Science, Sofia, Bulgaria*

basalts, the first group being silica over-saturated and the second - silica undersaturated[20].
The first group is typical for the re-fused rock industry[21]. Somewhat similar glass composition was also synthesised for nuclear waste immobilization[22] and for vitrification of hazardous industrial wastes[23-25].
The second group is characterized by a lower melting temperature and lower viscosity; for this reason it can be considered as more suitable for the ceramic industry.
In the present work a batch composition of 50 wt % basaltic tuffs and 50 wt % local industrial clays was investigated. The sintering behaviour was studied by hot-stage microscopy and dilatometry. The textures of the samples obtained at different temperatures were characterized by different picnometric techniques and observed by SEM.

2. Experimental

The tuffs were crushed and milled for 30 min in agathe mill and then sieved under 75 µm. The particles shape was observed by optical microscopy. The chemical analyses of the basaltic tuffs, parent clays and final ceramic were made by XRF analysis (Spectro XEPOS). The phase analyses of the tuffs were carried out by XRD (Philips PW1830 apparatus and CuK_{α} radiation) and by optical microscopy. The amount of amorphous fraction was estimated by comparing total areas of the crystalline phases with one of the amorphous phase in the XRD spectrum[26]. DTA analysis (Netzch STA 409) was performed on 100 mg powder sample by at 10 °C/min heating rate.
The batch was obtained by mixing 50 wt % tuffs, 30 wt % kaolinitic clays (labelled KC) and 20% illitic clays (labelled IC) with 8% water. Green samples were uniaxially pressed at 30 MPa .
The sintering behaviour was studied by hot-stage microscopy and by differential dilatometry (Netzch 402 ED) at 10 °C/min heating rate.
50 mm diameter and about 10 mm width green samples were fired at 900 °C, 1000 °C, 1100 °C and 1150 °C for 2h at heating and cooling rates of 10 °C /min. Water absorption, W, was evaluated after 2 h boiling at 100 °C. The bulk (apparent) density, ρ_b, was measured by a dry flow pycnometer (GeoPyc 1360)[14, 27]. The skeleton (relative), ρ_s, and real (absolute), ρ_r, densities were measured by He displacement Pycnometer (AccuPyc 1330)[14, 27] before and after milling the samples below 53 µm, respectively.
AccuPyc 1330 is a gas displacement Pycnometer, which determines the density by the change of He pressure in a calibrated volume.
For bulk samples the measured density corresponds to the sum of mass volume and closed for He pores; for powdered samples corresponds to the absolute density. GeoPyc 1360 measures the "enveloped" (bulk) volume of samples, placed in compressed free-flowing dry medium (named Dry Flow and made of tiny, rigid spheres).
The density results were used to determine total porosity, $P_T = 100*[(\rho_r - \rho_b)/\rho_r]$, closed porosity, $P_C = 100*[(\rho_r - \rho_s)/\rho_r]$, open porosity to He, $P_{He} = P_T - P_C$ and open porosity to water, $P_{H20} = W*P_A$.
The fractured surfaces of the samples, sintered at different temperatures, were studied by SEM (LEO 440 Scanning Electron Microscope).

Table 1. Chemical compositions of the raw materials and of the batch

Wt %	Basaltic tuffs	Illitic clay	Kaolinitic clay	Batch
SiO_2	44.07±0.07	52.50±0.09	55.0±0.08	51.0±0.08
Al_2O_3	14.51±0.04	25.12±0.06	30.21±0.06	18.5±0.07
TiO_2	3.06±0.01	0.72±0.02	1.52±0.03	2.00±0.04
Fe_2O_3	14.04±0.04	7.91±0.03	0.55±0.001	9.34±0.03
CaO	9.92±0.05	tr.	0.29±0.01	5.51±0.02
MgO	7.87±0.07	2.5±0.05	0.73±0.02	4.56±0.08
Na_2O	4.12± 0.17	0.40±0.02	3.26±0.13	3.52±0.04
K_2O	1.73±0.01	4.3±0.02	0.57±0.01	2.19±0.02

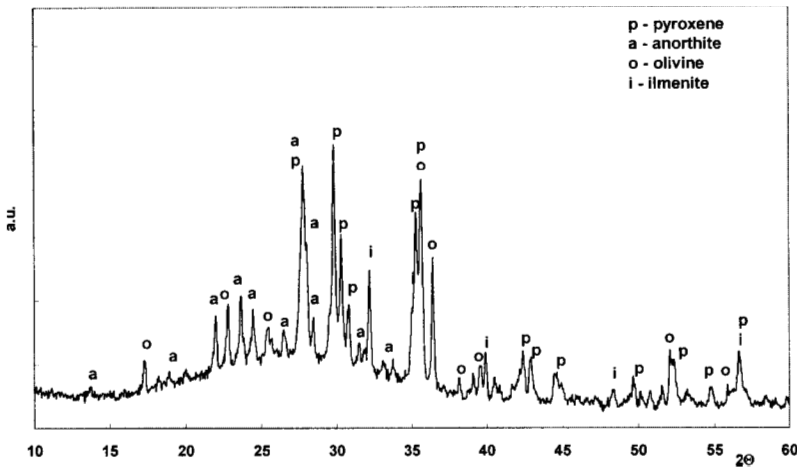

Figure 1. XRD spectra of the tuffs

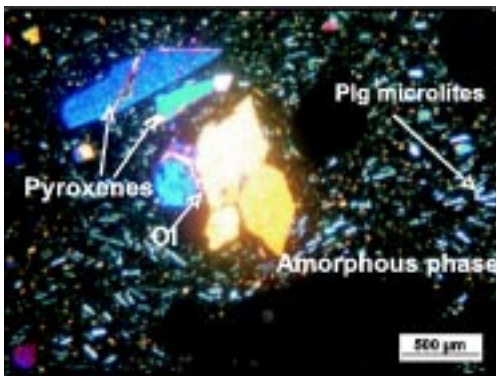

Figure 2. Optical microscopy of the tuffs

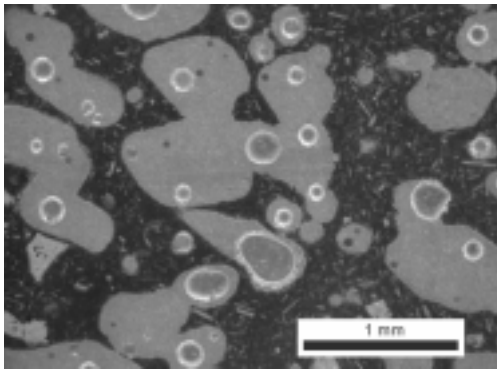

Figure 3. Thin section microscopy of the tuffs

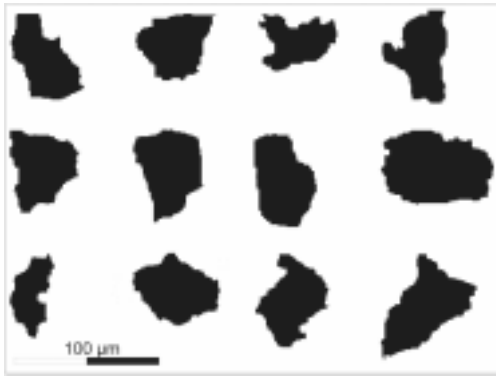

Figure 4. Microscopy of particles obtained after milling

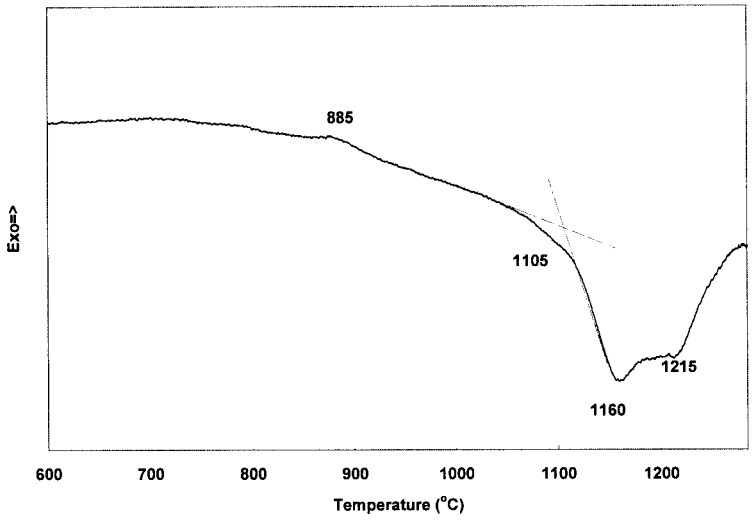

Figure 5. DTA of the tuffs

3. Results and discussion

3.1. Raw materials characteristics

The used basaltic tuffs are widespread in the Southern part of Turkey, while the clays are typical for the local ceramic industry. The chemical analyses are shown in Table 1. The tuff composition is typical for the alkaline basaltic rocks, kaolinitic clays contains higher Al_2O_3, while illitic clays contains higher iron oxides content.
Figure 1 shows the XRD spectra of the tuffs. It highlights a high amount of 50-60% amorphous phase, clino-pyroxene as main crystal phase and plagioclases (anorthite solid solution), olivine (forsterite solid solution) and ilmenite spinels as secondary phases. The elevate amount of glassy phase may be explained by the tuffs forming conditions (i.e. intensive eruption, followed by fast water or air cooling). On the contrary, the massive basaltic rocks, formed by lava flow and slow cooling, are characterized by higher crystallinity.
The XRD results were confirmed by optical microscopy. Figure 2 shows the prismatic pyroxene minerals with bluish-green colours, high relief olivines with active yellow colours, and felsic plagioclase microlites, embedded in the amorphous phase.
The used basaltic tuffs are characterized by 40-60% open porosity; as a result, the material is easily crushed and grinded. Figure 3 shows a thin section of the tuffs. Figure 4 shows the particles, obtained after crushing: the shapes (mostly subangular, semi-rounded and semi-spherical) are appropriate for the ceramic industry.
The DTA (Figure 5) highlights a low intensity exothermic effect at 885 °C due to secondary crystallization of the glassy phase, followed by endothermic effects in the range 1100-1250 °C due to intensive melting of the crystal phases. The peak at 1160 °C can be related to the melting of pyroxene while that at 1215 °C to the melting of the secondary phases[20, 21].

3.2. Sintering behaviour

Hot-stage microscopy (Figure 6) shows the beginning of sintering at about 1100 °C and of deformation after ~1200 °C. Due to the reduction of Fe^{+3} to Fe^{+2} and gas release, the deformation is accompanied with a volume increase. This phenomenon is common for ceramics with a high percentage of iron oxides[1, 3].
The densification behaviour was confirmed by the dilatometric results, shown in Figure 7. The traces highlight ~0.5% linear shrinkage in the range 985-1020 °C, due to the phase transformation of metakaolinite[14, 28] and beginning of sintering at 1105 °C. The deformation starts after 8% shrinkage at 1185 °C.
Table 2 reports the values of water absorption, apparent density, relative density and absolute density, obtained

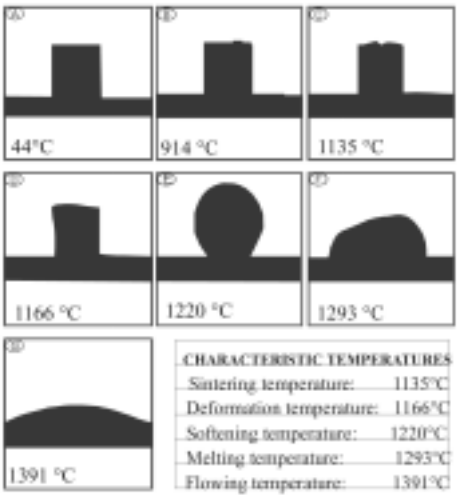

Figure 6. Hot-stage microscopy analysis of the ceramic sample

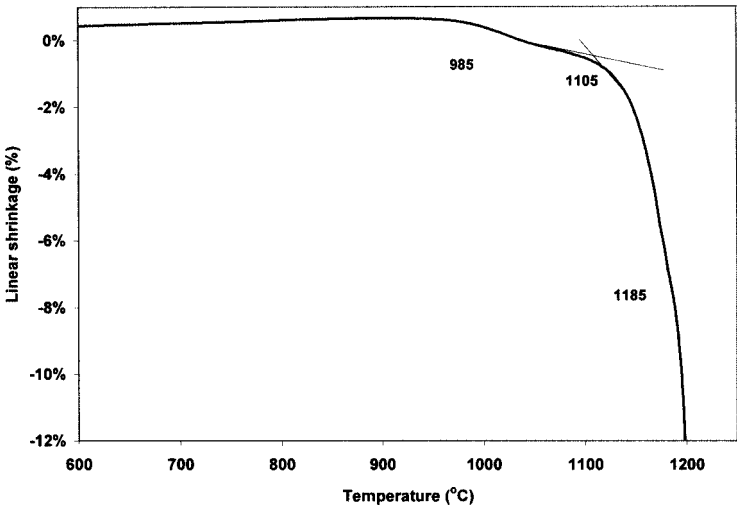

Figure 7. Dilatometry of the ceramic sample

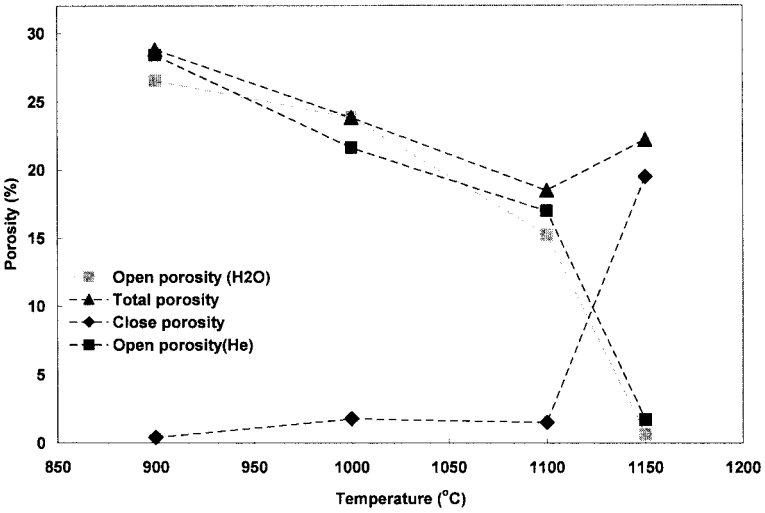

Figure 8. Total porosity (P_T), closed porosity (P_C) and open porosities for He (P_{He}) and water (P_{H2O}) after 2 h holding at different sintering temperatures

at different temperatures. Figure 8 shows the corresponding total porosity (P_T), close porosity (P_C), and open porosities for He (P_{He}) and water (P_{H2O}), respectively.

At 900 °C no significant densification occurs. At 1000 °C and 1100 °C P_T decreases but the porosity remains open with similar P_{He} and P_{H2O} values. An intensive sintering, leading to sample without open porosity, occurs at 1150 °C. The closed porosity of this sample, however, is too high which indicates an overfiring process.

The fractured surfaces of the sintered samples were studied by SEM. Figure 9-a confirms the scarce sintering at 900 °C. Figure 9-b highlights the beginning of the amorphous phase formation and densification at 1100 °C. Figure 9-c shows the structure at 1150 °C with typical amorphous fracture and new kind of cubic and fibre like crystals.

In order to reduce the overfiring effect, the sintering time at 1150 °C was shortened to 30 min; the obtained W, ρ_a, ρ_s and ρ_r are given in Table 2. The corresponding values of 13% total porosity and 4% water absorption are typical for the earthenware tiles, manufactured by similar production cycle[3].

The XRD analysis of the sample fired for 30 min is presented in Figure 10. 30-40% amorphous phase, quartz and anorthite plagioclases are the main phases, whereas orto-pyroxene, olivine, hematite and spinels are the secondary ones. The quartz comes from the clays while the olivine and spinels from the basaltic

Table 2. Water absorption, apparent density, skeleton density and absolute density at different temperatures

	W % (%)	ρ_a (g/cm³)	ρ_s (g/cm³)	ρ_r (g/cm³)
900 (2h)	13.61±0.06	1.95±0.016	2.73±0.004	2.74±0.003
1000 (2h)	11.19±0.05	2.11±0.014	2.72±0.003	2.77±0.002
1100 (2h)	6.96±0.04	2.24±0.013	2.71±0.004	2.75±0.003
1150 (2h)	0.32±0.05	2.03±0.015	2.14±0.005	2.66±0.002
1150 (0.5h)	3.86±0.04	2.32±0.014	2.61±0.003	2.72±0.003

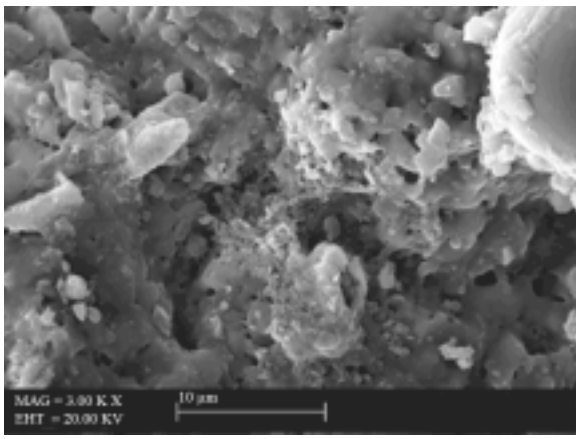

a)

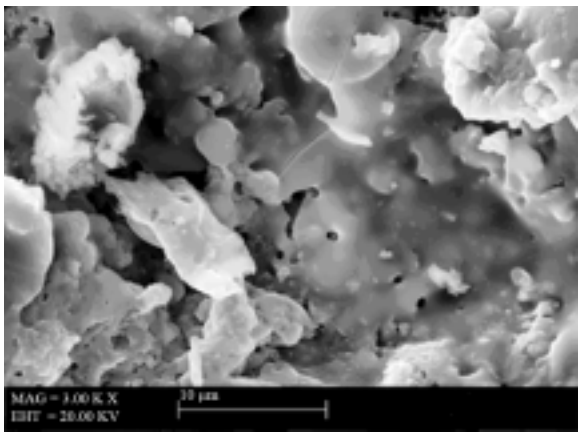

b)

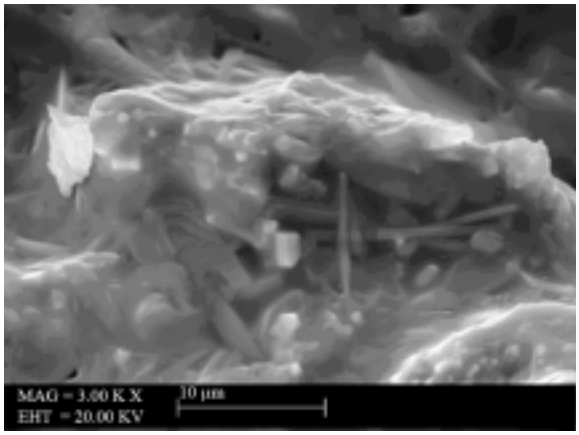

c)

Figure 9. Fracture images of samples, fired at 900 °C (a), 1100 °C (b) and 1150 °C (c)

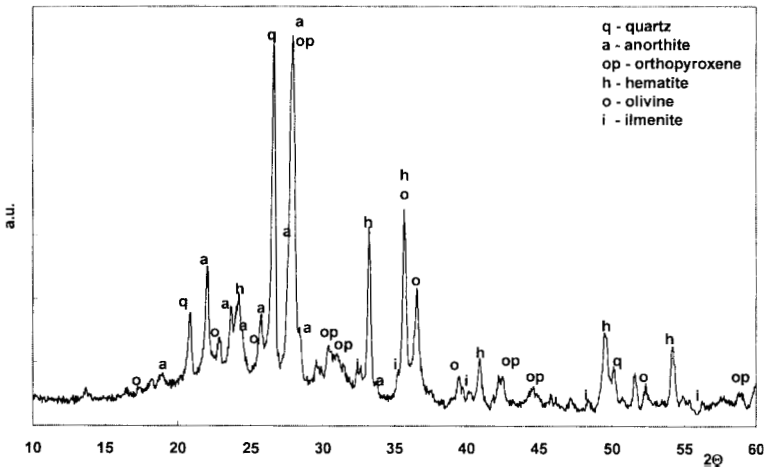

Figure 10. XRD analysis of the ceramic fired for 30 min at 1150 °C

tuff; the other phases form during sintering and cooling. Clino-pyroxene from the basaltic tuffs and metakaolinite (or mullite) from the clays are absent, which indicates that these phases melt and then participate in the formation of new plagioclase and orto-pyroxene phases. Similar re-crystallization processes are unusual for a quartz-feldspars-clays ceramic. In the common compositions the melt formed at sintering temperature solidifies in a glassy phase during cooling. As a result, the well sintered porcelain stoneware and tableware products contain high amount of amorphous phase[1, 3, 5, 14].

4. Conclusion

The used tuffs are characterised by a high amount of amorphous phase and high initial porosity; as a result they may be crushed and milled easily. The batch obtained by 50 wt % basaltic tuffs and 50 wt % industrial clays is characterized by a relatively short sintering range, corresponding to the melting range of the clino-pyroxene phase in the tuffs. Samples with 13% total porosity and 4% water absorption were obtained at 1150 °C for 30 min holding time. Due to an intensive re-crystallization of plagioclases and orto-pyroxene the ceramic is also characterized by high crystallinity.

Acknowledgment

The authors thank to Prof. Mario Pelino and Prof. Donatello Magaldi for the useful discussions and the technical support.

References

1. W.D. Kingery, Introduction to Ceramics, J. Wiley & Sons, New York, 1976.
2. J.S. Reed, Principles of Ceramic Proceedings, J. Wiley & Sons, New York, 1995.
3. J. Hlavac, The Technology of Glass and Ceramics: an Introduction, Elsevier, Amsterdam, 1983.
4. W.M. Carty, U. Senapati, Porcelain - Raw Materials,

Processing, Phase Evolution, and Mechanical Behavior, J. Am. Ceram. Soc. 81 (1) (1998) 3-20.
5. T. Manfredini, G. Pellacani, M. Romagnoli, L. Pennisi, Porcelainized Stoneware Tile, Am. Ceram. Soc. Bull. 74 (5) (1995) 76-79.
6. M.F. Abadir, E.H. Sallam, I.M. Bakr, Preparation of porcelain tiles from Egyptian raw materials, Ceram. Int. 28 (2002) 303-310.
7. R. Gennaro, P. Cappelletti, G. Cerri, M. Gennaro, M. Dondi, G. Guarini, A. Langella, D. Naimo, Influence of zeolites on the sintering and technological properties of porcelain stoneware tiles, J. Eur. Ceram. Soc. 23 (2003) 2237-2245.
8. K. Dana, S. Das, S. K. Das, Effect of substitution of fly ash for quartz in triaxial kaolin-quartz-feldspar system, J. European Ceram. Soc. 24 (2004) 3169-3175.
9. Tucci, L. Esposito, E. Rastelli, C. Palmonari, E. Rambaldi, Use of soda-lime scrap-glass as a fluxing agent in a porcelain stoneware tile mix, J. Eur. Ceram. Soc. 24 (2004) 83-92.
10. S.R. Bragança, C.P. Bergmann, Traditional and glass powder porcelain: Technical and microstructure analysis, J. Eur. Ceram. Soc. 24 (2004) 2383-2388.
11. F. Matteucci, M. Dondi, G. Guarini, Effect of soda-lime glass on sintering and technological properties of porcelain stoneware tiles, Ceram. Int. 28 (2002) 873-880.
12. P. Torres, H.R. Fernandes, S. Agathopoulos, D.U. Tulyaganov, J.M.F. Ferreira, Incorporation of granite cutting sludge in industrial porcelain tile formulations, J. Eur. Ceram. Soc. 24 (2004) 3177-3185.
13. F. Andreola, L. Barbieri, A. Corradi, I. Lancellotti, T. Manfredini, Utilisation of municipal incinerator grate slag for manufacturing of porcelainized stoneware tiles manufacturing, J. Eur. Ceram. Soc. 22 (2002) 1457-1462.
14. A. Karamanov, E. Karamanova, A.M. Ferrari, F. Ferrante, M. Pelino, The effect of scrap addition on the sintering behavior of hard porcelain, Ceram. Int., 32 (2006) 727-732.
15. S. Ergun, M. Akyildiz, S. Necdet, The Use of Basaltic Tephra In Ceramic Slurry as an Unsticky Raw Material and Impacts on Rheology, 13th Clay Symposium, Van, Turkey, 528-535, 2005.
16. N. Sakarya, S. Kapur, E.A. FitzPatrick, Preliminary study of the microstructure and minerology of 12th and 13th century ceramics, Samsat, Southeastern Turkey. Geoarchaelogy, 5 (1990) 275-281.
17. S. Kapur, N. Sakarya, E.A. FitzPatrick, Minerology and micromorphology of 16th and 17th Century Iznik Ceramics. Proceedings of International Symposium of Iznik Ceramics, Istanbul, Turkey, 237-241,1990.
18. O. Parlak, H. Kozlu, C. Demirkol, M. Delaloye, Intracontinental Plio-Quaternary volcanism along the African-Anatolian plate boundary, Southern Turkey, Ofioliti 22 (1997)111-117.
19. K. Notsu, T. Fujitani, T. Ui, J. Matsuda, T. Ercan, Geochemical features of collision-related volcanic rocks in central and eastern Anatolia, Turkey, J. Volcanol. Geotherm. Res. 64 (1995) 171-192.
20. S.A. Morse, Basalts and Phase Diagrams, Springler-Verlag, New York, Heidelberg, Berlin, 1982.
21. B. Locsei, Molten Silicates and their Properties, Akademiai Kiado, Budapest, 1970.
22. I.W. Donald, B.L. Metcalfe and R.N.J. Taylor, "Review- The Immobilization of high level radioactive wastes using ceramics and glasses", J. Material Sci. 32, (1997), 5851-5887.
23. M. Romero, J. Ma. Rincon, Preparation and Properties of High Iron Oxide Content Glasses Obtained from Industrial Wastes, J. European Ceram. Soc, 18 (1998) 153-160.
24. A. Karamanov, M. Pelino, Crystallization Phenomena in Iron Rich Glasses, J. Non-Crystalline Solids, 281 (2001) 139-151.
25. A. Karamanov, G. Taglieri, M. Pelino, Sintering in nitrogen atmosphere of iron-rich glass-ceramics, J. American Cer. Soc., 87 (2004) 1354-1357.
26. H.P. Klug, L.E Alexander, X-ray Diffraction Procedures for Polycrystaline and Amorphous Materials, John Wiley & Sons, New York, 1974.
27. http://www.micromeritics.com
28. J. Blumm, Recent Advanced in Dilatometry, Am. Ceram. Soc. Bull. 79 (11) (2000) 64-68.